

1 **Supplementary Information**

2 **Local artifacts in ice core methane records caused by layered bubble** 3 **trapping and in-situ production: a multi-site investigation**

4 **R. H. Rhodes et al.**

5

6 **1. Additional information about processing of the continuous CH₄ data**

7 Methane concentrations measured by the SARA laser spectrometer were transferred to
8 the NOAA2004 scale by measuring three NOAA-certified reference gases (CA04382 =
9 385 ppb, CA04332 = 667 ppb and CC302559 = 1853 ppb). Measurements conducted in
10 September 2013 were calibrated using equation 1.

$$11 \text{CH}_{4\text{NOAA2004}} = 1.0127 * \text{CH}_{4\text{meas.}} - 1.4201 \quad 1)$$

12 Measurements conducted in October 2013 were calibrated using equation 2.

$$13 \text{CH}_{4\text{NOAA2004}} = 0.9878 * \text{CH}_{4\text{meas.}} + 5.0957 \quad 2)$$

14 Different calibrations were applied in September and October because maintenance was
15 carried out on the instrument between measurement sessions. Please see Table S1 for
16 analysis dates.

17 NOAA-calibrated methane concentrations were corrected for dissolution in the liquid
18 phase using measurements made on a synthetic sample mixture of reference gas and
19 degassed water as described previously (Rhodes et al., 2015, 2013). Each core or
20 analytical batch has a unique solubility correction to account for differences in system
21 parameters, particularly melt rate and degasser used (Table S1).

22 **2. Modifications to Oregon State University (OSU) discrete CH₄ analysis**

23 A minor change to the methods reported by Mitchell et al. (2011) relates to the
24 application of solubility and blank corrections to discrete CH₄ measurements conducted
25 at OSU. As detailed by Mitchell et al. (2011), the blank correction is determined by
26 adding a known pressure of standard gas over ultra pure air-free ice (AFI). The measured
27 deviation in CH₄ concentration from a calibrated standard gas (500.22 ppb) comprises the

1 blank correction. The solubility correction (SC) is determined by performing a secondary
2 melt-refreeze cycle. The high solubility of CH₄ relative to N₂ results in a CH₄ depletion
3 in the the measured sample. We have modified how these corrections are applied.
4 Previously, corrected CH₄ (CH_{4 cor}) values were calculated using equation 3.

$$5 \text{ CH}_{4 \text{ cor}} = (\text{CH}_{4 \text{ sample}} - \text{CH}_{4 \text{ blank}}) * \text{SC} \quad 3)$$

6 This calculation underestimates the solubility effect on the blank, and therefore ultimately
7 also underestimates CH_{4 cor}. The revised calculation fully accounts for the solubility
8 effect on the blank and sample measurements (eq. 4).

$$9 \text{ CH}_{4 \text{ cor}} = (\text{CH}_{4 \text{ sample}} * \text{SC} - \text{CH}_{4 \text{ AFI}}) * -\text{CH}_{4 \text{ standard}} \quad 4)$$

10 CH_{4 AFI} values on the OSU system are typically 505 ppb, meaning that measurements
11 corrected using equation 4 (as this study) are 8.5 ppb higher than those corrected using
12 equation 3.

13 **3. Splicing of Tunu13 Main and Tunu13 B records**

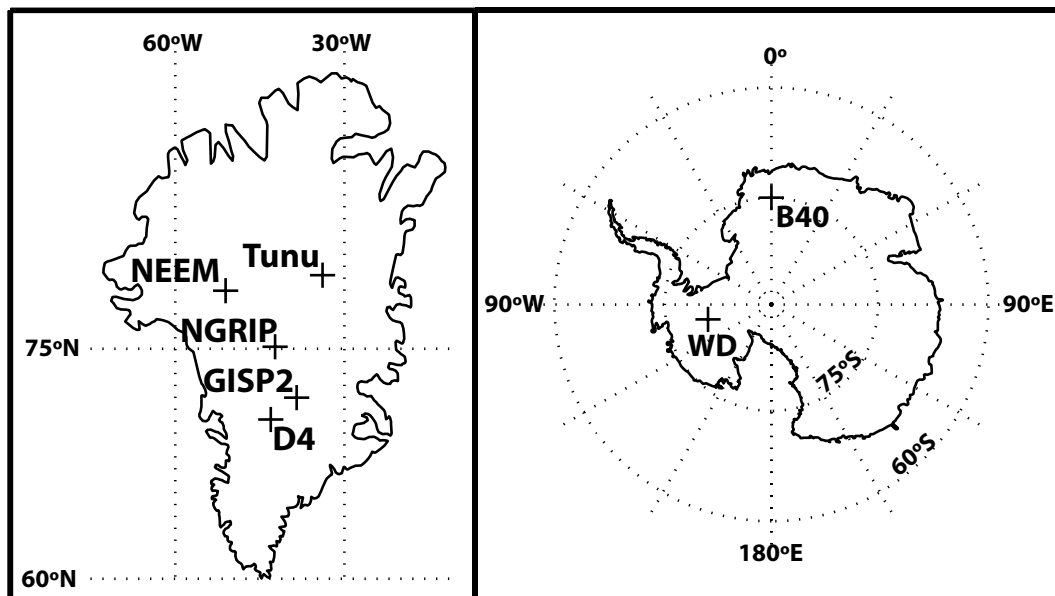
14 Ice from Tunu13 B core was analysed instead of Tunu13 Main core for sections with
15 poor Main core quality. Tunu13 B core CH₄ and chemistry data are spliced into the
16 Tunu13 Main record for the following depth ranges: 139.9–136.3 m, 131.5–128.6 m,
17 128.0–120.4 m & 105.2–99.63 m. Comparison between Tunu13 Main and B chemistry
18 records suggested that there was a 40 cm depth offset between the two cores. All Tunu13
19 B core depths were increased by 40 cm before splicing the CH₄ and chemistry data into
20 the Tunu13 Main record.

21 **4. Calculation of peak-to-peak amplitude**

22 The peak-to-peak amplitude of the high frequency CH₄ residual was calculated using a
23 publically available Matlab function called Peakdet (eq. 5).

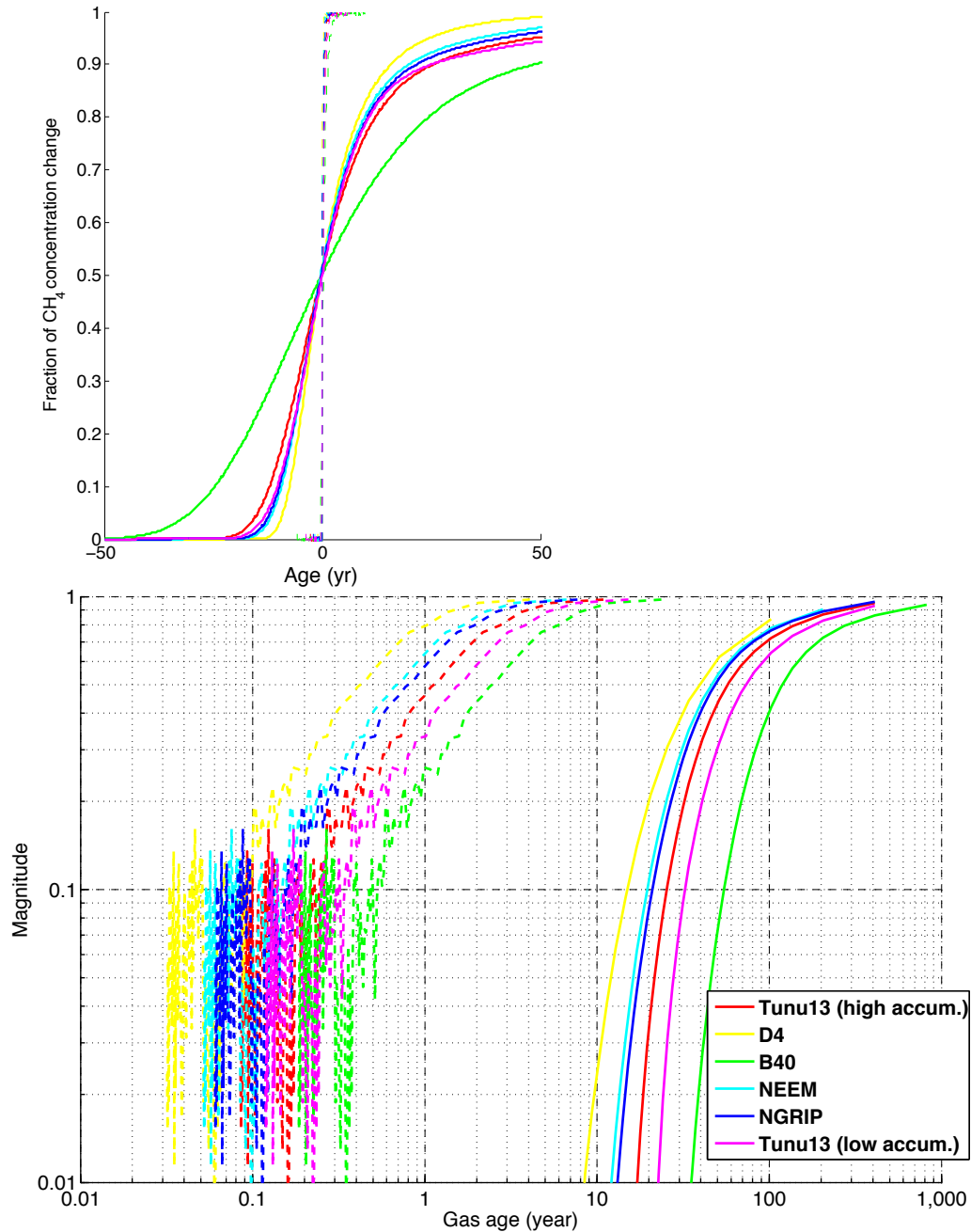
$$24 [\text{MAXTAB}, \text{MINTAB}] = \text{PEAKDET}(\text{V}, \text{DELTA}) \quad 5)$$

25 This function finds the local minima and maxima in the vector V. A data point is
26 considered to be a maximum if it is the highest value and was preceded by a values lower
27 by >=DELTA. DELTA is set to 2 ppb, slightly greater than the 2σ internal precision.



1

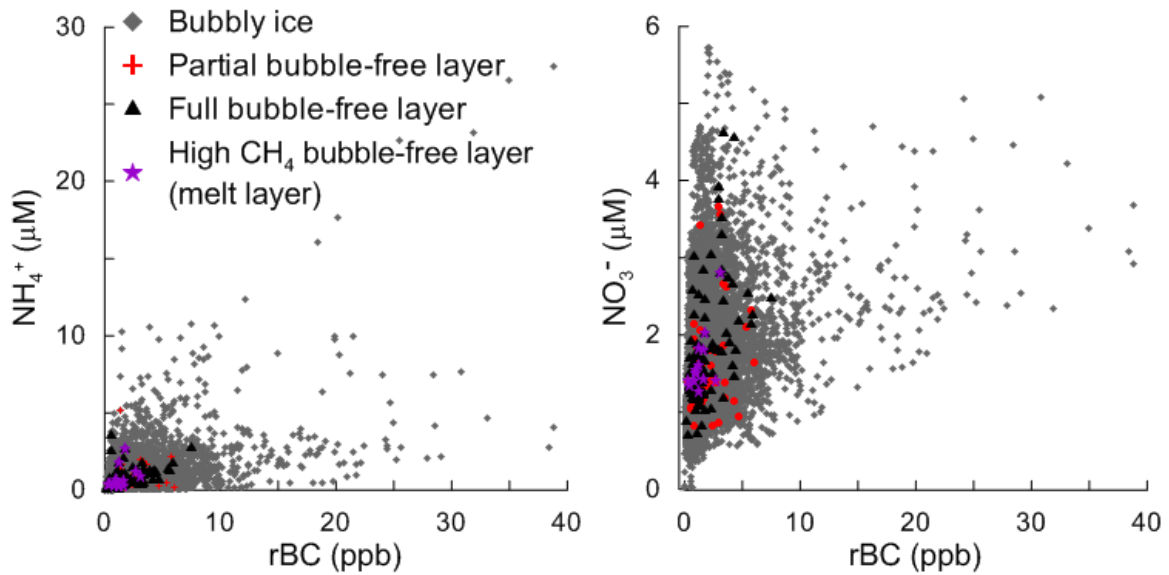
2 Figure S1: Locations of ice cores analyzed in study or referred to in the text. Greenland on
 3 left panel: Tunu(13) (78.035°N, 33.879°W), 2,200 m elevation; North Greenland Eemian
 4 (NEEM) (77.45°N, 51.06°W), elevation 2,450 m; North Greenland Ice Sheet Project
 5 (NGRIP) (75.10°N, 42.32°W), elevation 2,917 m; Greenland Ice Sheet Project 2 (GISP2)
 6 (72.60°N, 38.5°W), 3207 m elevation; D4 (71.40°N, 43.08°W), elevation 2,713 m.
 7 Antarctica on right panel: B40 (75.001°S, 0.068°E) , 2911 m elevation, West Antarctic Ice
 8 Sheet Divide (WD) (79.47°S, 112.08°W), 1766 m elevation.



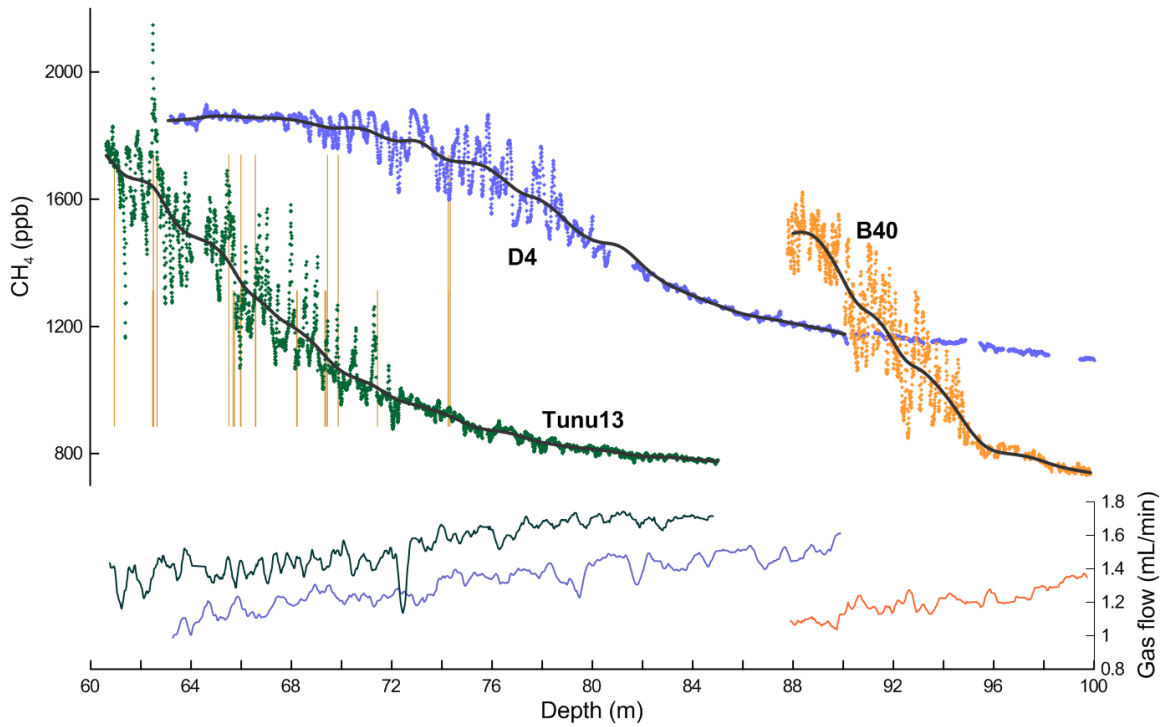
1 Figure S2: Upper panel) Relative smoothing of the analytical system (dashed lines) and
 2 firn-based processes (solid line) for each ice core (see legend). Lower panel) Bode
 3 magnitude plot showing magnitude of frequency response to filters representative of
 4 analytical system and firn smoothing for different ice cores. If we assume that CH₄
 5 variability is present in the ice cores at a 1 yr periodicity, the fraction of the original
 6 amplitude of that signal remaining after damping by the analytical system can be estimated

1 from this figure as: 0.4 for Tunu13 high accumulation, 0.8 for D4, 0.2 for B40, 0.65 for
2 NEEM, 0.57 for NGRIP and 0.35 for Tunu13 low accumulation.

3

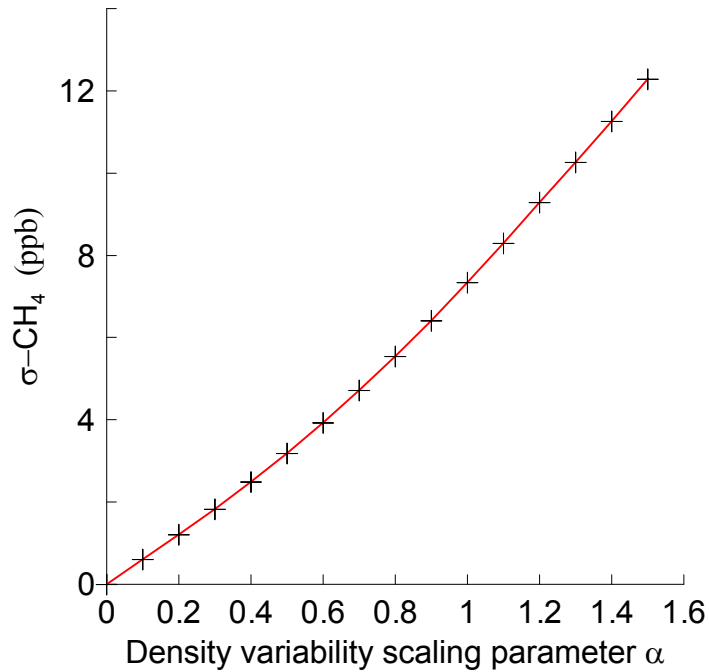


1
 2 Figure S3: Bi-plots to compare chemical concentrations in Tunu13 ice core at depths
 3 coincident with a full bubble-free layer (present across the melter stick surface area), partial
 4 bubble-free layer (present across part of melter stick surface area), bubble-free layers with
 5 anomalously high CH₄ (continuous and discrete data) concentrations, and depths of bubbly
 6 ice with no observed layers. Refractory black carbon (rBC), nitrate (NO₃⁻) and ammonium
 7 (NH₄⁺) are plotted. Bubble-free layers may be melt layers or wind crusts and it is difficult
 8 to distinguish between the two by eye.



1

2 Figure S4: Lock-in zone CH₄ data for Tunu13 (green), D4 (violet) and B40 (orange) with
 3 cubic spline fits (black). Gas sample flow recorded by the laser spectrometer is also shown
 4 for each core. Vertical brown lines through Tunu13 data show position of melt layers.
 5 Abrupt increase in amplitude of signal variability indicates location of close-off depth in
 6 each core.



1

2 Figure S5: Relationship between magnitude of density variability (α) and high frequency
 3 CH_4 variability ($\sigma\text{-CH}_4$) as predicted by the CIC firm air transport model for the WAIS
 4 Divide ice core. The scaling factor (α) applied to the WAIS Divide high resolution density
 5 information used by the model is varied between 0 and 1.6. When $\alpha=1$ the density is not
 6 modified. A growth rate of 2.5 ppb yr^{-1} and an accumulation rate of $0.22 \text{ m (ice) yr}^{-1}$ are
 7 assumed.

Table S1: Online system operating parameters and system performance. Please refer to footnotes for explanation.

Ice core	Analysis dates	Depth interval (m)	Mean melt rate (cm/min)	Mean (gas) sample flow (sccm)	Melter-head	Degasser	System response time (cm)	Solubility correction	Breaks/m (mean ± s.d)**
B40	11-13/09/13	200–122	5.54	1.59	Standard	M	9.4	$CH_4cor=(7^{-6}*CH_{4NOAA}^2)+(1.086*CH_{4NOAA})$	1.4 ± 0.4
	16-17/09/13	122–88	5.54	1.30	Standard	IL		$CH_4cor=(2^{-5}*CH_{4NOAA}^2)+(1.085*CH_{4NOAA})$	
	18/09/13	157–148	5.86	1.35	Standard	IL			
D4*	7-9/08/13	146–61	7.62	1.54	Small	M	13.0	$CH_4cor=1.1062*CH_{4NOAA}$	0.6 ± 0.3
	15/08/13	145–123		1.54	Small	M			
NEEM	3-6/09/13	573–491, 444–399	5.70	1.88	Standard	M	9.7	$CH_4cor=(1^{-5}*CH_{4NOAA}^2)+(1.069*CH_{4NOAA})$	1.9 ± 0.7
	7-8/10/13	491–444	5.70	1.76	Standard	IL		$CH_4cor=(4^{-6}*CH_{4NOAA}^2)+(1.114*CH_{4NOAA})$	
NGRIP	30/09-	254–207, 108–91	5.72	1.37	Dual ring	IL	9.7	$CH_4cor=(1^{-5}*CH_{4NOAA}^2)+(1.119*CH_{4NOAA})$	2.1 ± 0.6
	4/10/13	569–519			Dual ring	IL			
	08/31/13	91–74			Standard	IL			
Tunu13	13-21/08/13	213–73	5.94	1.8	Standard	M	10.1	$CH_4cor=(1^{-5}*CH_{4NOAA}^2)+(1.069*CH_{4NOAA})$	1.6 ± 1.6

* Only D4 data analysed on 07/08/2013 from 126.4–129.2 m depth are used. All other D4 data from this date are not used in this study.

**Values are mean #breaks/m calculated for each day of analysis. Individual metre-lengths of ice core may have contained more or less breaks.

Melterhead: Three different styles were used: standard = as McConnell et al. (2002); small = smaller cross-sectional area; dual ring = new design with two concentric sample rings available for gas sampling.

Degasser: M=Membrana Liqui-cel Micromodule; IL=IDEX inline degasser.

System response time: Time taken for CH₄ concentration to change between 10 and 90 % of total normalized concentration change resulting from switch between two different air standards mixed with degassed water and circulated through the analytical system (to mirror the pathway of the ice core sample). This value is converted to a depth using the melt rate.

Table S2: Bubble-free layers in Tunu13 ice cores associated with anomalously high CH₄ signals and assumed to be melt layers

Bottom depth (m)	Thickness (mm)	Excess CH₄ (ppb peak height)	Continuous or discrete CH₄ anomaly?	High CO?	Main or B core?
100.065	10	40	Contin.	Y	B
100.095	<5				
100.135	<5				
100.17	<5				
103.65	<5	15	Contin.	Y	B
103.465	<5				
103.47	<5				
108.855	<5	15	Contin.	Y	Main
112.48	<5	60	Contin.	Y	Main
112.515	5				
113.925	<5	30	Discrete	nd	Main
152.76	<5	40	Contin.	Y	Main
153.29	<5	10	Discrete	N	Main
156.31	<5	25	Discrete	N	Main
180.66	<5	30	Contin.	Y	Main
180.68	<5				
181.75	<5	15	Discrete	nd	Main
194.62	20	20	Discrete	Y	Main
194.625	<5				
201.35	<5	80	Contin.	Y	Main

nd=no data

References

- McConnell, J.R., Lamorey, G.W., Lambert, S.W., Taylor, K.C., 2002. Continuous ice-core chemical analyses using inductively coupled plasma mass spectrometry. *Environ. Sci. Technol.* 36, 7–11. doi:10.1021/es011088z
- Mitchell, L.E., Brook, E.J., Sowers, T., McConnell, J.R., Taylor, K., 2011. Multidecadal variability of atmospheric methane, 1000-1800 C.E. *J. Geophys. Res.* 116, doi:10.1029/2010JG001441. doi:10.1029/2010jg001441
- Rhodes, R.H., Brook, E.J., Chiang, J.C., Blunier, T., Maselli, O.J., McConnell, J.R., Romanini, D., Severinghaus, J.P., 2015. Enhanced tropical methane production in response to iceberg discharge in the North Atlantic. *Science* 348, 1016–1019.
- Rhodes, R.H., Faïn, X., Stowasser, C., Blunier, T., Chappellaz, J., McConnell, J.R., Romanini, D., Mitchell, L.E., Brook, E.J., 2013. Continuous methane measurements from a late Holocene Greenland ice core: Atmospheric and in-situ signals. *Earth Planet. Sci. Lett.* 368, 9–19. doi:10.1016/j.epsl.2013.02.034